

Isotocin controls ion regulation through regulating ionocyte progenitor differentiation and proliferation

Ming-Yi Chou · Jo-Chi Hung · Liang-Chun Wu ·
Sheng-Ping L. Hwang · Pung-Pung Hwang

Received: 1 June 2010/Revised: 31 October 2010/Accepted: 5 November 2010/Published online: 24 November 2010
© The Author(s) 2010. This article is published with open access at Springerlink.com

Abstract The present study using zebrafish as a model explores the role of isotocin, a homolog of oxytocin, in controlling ion regulatory mechanisms. Double-deionized water treatment for 24 h significantly stimulated isotocin mRNA expression in zebrafish embryos. Whole-body Cl^- , Ca^{2+} , and Na^+ contents, mRNA expressions of ion transporters and ionocyte-differentiation related transcription factors, and the number of skin ionocytes decreased in isotocin morphants. In contrast, overexpression of isotocin caused an increase in ionocyte numbers. Isotocin morpholino caused significant suppression of *foxi3a* mRNA expression, while isotocin cRNA stimulated *foxi3a* mRNA expressions at the tail-bud stage of zebrafish embryos. The density of P63 (an epidermal stem cell marker)-positive cells was downregulated by isotocin morpholinos and was upregulated by isotocin cRNA. Taken together, isotocin stimulates the proliferation of epidermal stem cells and differentiation of ionocyte progenitors by regulating the

P63 and *Foxi3a* transcription factors, consequently enhancing the functional activities of ionocytes.

Keywords Isotocin · Ionocyte · Zebrafish · Ion · Differentiation

Introduction

Oxytocin and vasopressin are structurally related neurohypophysial hormones in mammals [1, 2]. Isotocin and vasotocin are teleost homologues of mammalian oxytocin and vasopressin, respectively [1, 2]. According to a study on Fugu genomic organization, vasotocin/isotocin locus suggests that the two genes have evolved from a common ancestor through tandem duplication, and that this locus may have undergone a localized reorganization during vertebrate evolution [2]. Both oxytocin and isotocin stimulate contractions of smooth muscles and influence several behavioral and physiological processes such as social, sexual, and maternal behaviors, learning, memory, and parturition [3–5]. As for other physiological events, oxytocin and isotocin were demonstrated to regulate body fluids. Several studies suggested that dehydration or salt-loading resulted in increases in the transcription of the oxytocin gene and the proportion of neurons expressing oxytocin [6]. Oxytocin was assumed to directly act on the right atrium to stimulate atrial natriuretic peptide release, which acts to reduce the water, sodium, and adipose loads on the circulatory system, thereby reducing blood pressure [7].

Isotocin (isotocin-neurophysin, *itnp*) was also proposed to be associated with the internal osmotic and ionic homeostasis in fish. Transfer from fresh water to seawater stimulated the plasma concentration of isotocin, suggesting

M.-Y. Chou and J.-C. Hung contributed equally to this work.

M.-Y. Chou · J.-C. Hung · L.-C. Wu · S.-P. L. Hwang ·
P.-P. Hwang (✉)
Institute of Cellular and Organismic Biology, Academia Sinica,
Nankang, Taipei 11529, Taiwan
e-mail: pphwang@gate.sinica.edu.tw

M.-Y. Chou
e-mail: eleber@gate.sinica.edu.tw

J.-C. Hung
e-mail: roche@gate.sinica.edu.tw

L.-C. Wu
e-mail: r98b45008@ntu.edu.tw

S.-P. L. Hwang
e-mail: zoslh@gate.sinica.edu.tw

its involvement in osmoregulation of teleostean fish [8–11]. On the contrary, isotocin receptor was not well known to date. Isotocin receptor is expressed in many tissues including brain, gill, liver, spleen, heart, bladder, muscle, and kidney in teleost fish [12]. A study in eel indicated that upper esophageal sphincter muscle possesses isotocin receptor, which causes muscle relaxation and controls drinking behavior by enhancing cAMP production [13]. Studies of both mammals and fish suggested that oxytocin and isotocin are associated with hydromineral homeostasis of body fluids; however, our understanding of the physiological roles of oxytocin and isotocin in vertebrate ion- and osmoregulation is still fragmentary and needs further elucidation. The mechanisms behind these regulatory functions, including the target cells of oxytocin/isotocin, are still unclear.

Recently, oxytocin was suggested to be a growth and cell differentiation factor [14]. Oxytocin stimulates the proliferation of thymocytes [15] and enhances myoepithelial cell differentiation and proliferation in the mouse mammary gland [16]. The carboxyl terminally extended oxytocin precursor peptide induces embryonic stem cell-derived cardiomyogenesis and increases spontaneous beating activity [17]. During bone formation, oxytocin stimulates the differentiation of osteoblasts [18]. On the other hand, ionocytes in the skin/gills are the main cells responsible for fish ionoregulatory mechanisms, and the regulation of ionocyte functions was proposed to be mediated by the proliferation and differentiation of ionocytes [19, 20]. At least three subtypes of ionocytes were found in zebrafish skin/gills: $\text{Na}^+\text{-K}^+\text{-ATPase}$ -rich cell (NaRC), $\text{H}^+\text{-ATPase}$ -rich cell (HRC), and $\text{Na}^+\text{-Cl}^-$ cotransporter cell (NCC), which are responsible for calcium uptake, acid/base balance, and chloride uptake, respectively [21–24]. In addition, several transcription factors that are related to ionocyte differentiation have been identified. The interaction between forkhead box transcription factors, Foxi3a and Foxi3b, was demonstrated to control NaRC and HRC differentiation [25–28]. Recently, another transcription factor, glial cell missing homolog 2 (Gcm2), was identified to specifically influence differentiation and maturation of HR cells [27, 29]. When zebrafish embryos are acclimated to acidic environments, the number of HR cells increases, causing enhancement of the acid-secreting function [30]. Similarly, the number of epithelial calcium channel (ECaC)-expressing cells (a subtype of NaRC) and *ecac* messenger (m)RNA expression were elevated after low- Ca^{2+} treatments [21]. Taking those results into consideration, we hypothesized that isotocin may modulate the proliferation and differentiation of ionocytes to control ionoregulatory mechanisms.

Zebrafish (*Danio rerio*) have a similar body plan and essentially the same organ systems as humans [31], and the functions of zebrafish genes can be easily evaluated in vivo

by overexpression and antisense morpholino oligonucleotide-mediated knockdown experiments in embryos and larvae. The ionoregulatory mechanisms of zebrafish were recently well studied. According to serial molecular physiological studies, a working model of ionoregulatory mechanisms in the skin and gills of zebrafish, and the molecular physiological approaches to understand fish ion regulation and the controlling pathways were accordingly established [19, 32, 33]. Therefore, zebrafish are suitable to provide a platform to study the hormone control of ionoregulatory mechanisms. In the present study, we used zebrafish as a model to investigate the roles of isotocin on ionoregulatory mechanisms. Isotocin mRNA expression was induced by hypotonic stimulation. Knockdown of isotocin retarded whole-body ion contents, ionocyte-related gene expressions, and ionocyte densities; while overexpression of isotocin caused an increase of ionocyte cell numbers. Moreover, isotocin morphants showed lower *foxi3a* (a transcriptional factor controlling ionocyte differentiation) [25–28, 34] expression level at the tail-bud stage and a decrease in P63 (an epidermal stem cell marker) [35, 36] expression; while injection of isotocin capped-mRNA stimulated *foxi3a* and P63 expressions, suggesting that isotocin is involved in the differentiation and proliferation of ionocyte progenitors. Our results elucidate a molecular/cellular pathway of isotocin control in ionoregulatory mechanisms and provide new insights into this issue.

Materials and methods

Experimental fish

The AB strain of zebrafish (*Danio rerio*) were obtained from the stock of the Institute of Cellular and Organismic Biology, Academia Sinica, and mature fish were raised in a circulating system at 28°C under an illumination cycle of 14/10 h of a light/dark photoperiod. Embryos were also allowed to develop at 28°C. For hypotonic treatments, embryos were incubated in double-deionized water (Milli-RO60; Millipore, Billerica, MA, USA) for 72 h (for measurement of Ca^{2+} and Na^+ contents) or incubated in local tap water for 72 h and then transferred to double-deionized water for another 24 h (for detection of the *itnp* mRNA expression level). Experiments were performed in accordance with guidelines of the Academia Sinica Institutional Animal Care and Utilization Committee (approval no. RFiZOOHP2007086).

Preparation of total RNA

In order to obtain a sufficient quantity of RNA, 30 embryos or adult zebrafish tissues dissected from six individuals

were pooled as a sample. Samples were homogenized in 0.8 ml Trizol Reagent (Invitrogen, Carlsbad, CA). After chloroform extraction, the total RNA samples were purified and treated with DNaseI to remove the genomic DNA using an RNeasy Mini Kit (Qiagen, Huntsville, AL). The quantity and quality of total RNA were, respectively, assessed by Nanodrop spectrophotometry (ND-1000, NanoDrop Technology, Wilmington, DE, USA) and agarose gel electrophoresis.

Reverse-transcription polymerase chain reaction (RT-PCR) analysis

For cDNA synthesis, 5 µg of total RNA was reverse-transcribed in a final volume of 20 µl containing 0.5 mM dNTPs, 2.5 µM oligo(dT)₂₀, 250 ng of random primers, 5 mM dithiothreitol, 40 units of an RNase inhibitor, and 200 units of PowerScript reverse transcriptase (Invitrogen) for 30 min at 50°C, followed by incubation at 70°C for 15 min. Then, 20 units *Escherichia coli* RNase H (Invitrogen) was added to remove the remnant RNA in a 20-min incubation at 37°C. For PCR amplification, 1 µl of cDNA was used as a template in a 25-µl final reaction volume containing 0.25 µM dNTP, 1.25 units of Gen-Tag polymerase (Genemark, Taipei, Taiwan), and 0.2 µM of each primer. The primer sets are shown in Table 1.

Quantitative (q)RT-PCR

mRNA expression levels of ionocyte-related genes, such as forkhead box I3a (*foxi3a*, NM_198917), Na⁺-K⁺ ATPase, beta 1b polypeptide (*atp1b1b*, NM_131671), epithelial Ca²⁺ channel (*trpv6*, NM_001001849), H⁺-ATPase subunit A (*atp6v1a*, NM_201135), the Na⁺-Cl⁻ cotransporter (*slc12a10.2*, NM_001045001), Na⁺/H⁺ hydrogen

exchanger 3b (*nhe3b*, EF591980.1), and isotocin (*itnp*, AY069956) were measured by a qRT-PCR with a Roche Lightcycler 480 (Roche, Penzberg, Germany). The final volume in a well was 10 µl, and contained 5 µl of 2× SYBR green master mix (Roche), 3.2 ng of cDNA, and 50 nM of primer pairs. The standard curve of each gene was checked in the linear range with β -actin, elongation factor 1-alpha (EF1a), and ribosomal protein L13a (RPL13a) as internal controls. For the qRT-PCR experiments, normalization using three reference genes showed similar patterns; therefore, only data normalized to β -actin are shown in the present study. Primers were designed using Primer Express 2.0 software (Applied Biosystems, Wellesley, MA, USA). The primer sets are given in Table 1.

Whole-body Na⁺, Ca²⁺, and Cl⁻ contents

Fifteen zebrafish larvae were briefly rinsed in deionized water and then pooled as one sample. HNO₃ at 13.1 N was added to the samples for digestion at 60°C overnight. Digested solutions were diluted with double-deionized water, and the total Na⁺ and Ca²⁺ contents were measured by atomic absorption spectrophotometry (Z-8000; Hitachi, Tokyo, Japan). For Cl⁻ content measurements, samples were homogenized with 1 ml deionized water and centrifuged at 14,000 rpm for 30 min. The supernatant was collected, and thereafter Hg(SCN₄)₂ (0.3 g in 95% ethanol) and NH₄Fe(SO₄)₂·12 H₂O (30 g in 135 ml 6 N HNO₃) solutions were added for the analysis. The Cl⁻ concentration was measured by the ferricyanide method with a double-beam spectrophotometer (model U-2000; Hitachi). Measurements of standard solutions of Na⁺, Ca²⁺, and Cl⁻ from Merck (Darmstadt, Germany) were used to make the standard curves.

Table 1 Specific primer sequences for RT-PCR and qRT-PCR

Gene name	Forward primer sequences (5′–3′)	Reverse primer sequences (5′–3′)
<i>β-actin</i>	ATTGCTGACAGGATGCAGAAG	GATGGTCCAGACTCATCGTACTC
<i>itnp</i>	GTCAATCAACCGGCCAACAG	GGGTGGCGAGTCGTGTG
<i>itnpr1</i>	ACGCCCTTCTTCTTCGTTTCAG	TATTTCTCCAGTGCCTCTTACAGC
<i>itnpr2</i>	TTCAGCATCCCCGAGGTTTA	GCACTGGTCCCTCTTCGTCTT
<i>atp6v1a</i>	GAGGAACCACTGCCATTCCA	CAACCCACATAAATGATGACATC
<i>atp1b1b</i>	CCAGGGTTTAATTTGGGCTG	GTTTGGGATCATTGTCTTGCTG
<i>gcm2</i>	TCCCTGTGGTTATGACTTTGCA	TGGACTTGAGCCATGAGACACT
<i>foxi3a</i>	CTCTCGTCAATGACTGCTTC	CAGCCTGAGAGTCCGACTTTC
<i>trpv6</i>	TCCTTCCCATCACCTCT	GCACTGTGGCAACTTTCGT
<i>slc12a10.2</i>	GCCCCAAAGTTTTCAGTT	TAAGCACGAAGAGGCTCCTTG
<i>ef1a</i>	CTGGAGGCCAGCTCAAACAT	ATCAAGAGTAGTACCGCTAGCATTAC
<i>rpl13a</i>	CCTCGGTCGTCTTCCGCTATTG	CAGCCTGACCCTCTTGTTTGG
<i>nhe3b</i>	TGCAGACAGCGCCTCTAGC	TGTGGCCTGTCTCTGTTTGC

Translational knockdown with antisense morpholino oligonucleotides (MOs)

The morpholino-modified antisense oligonucleotide was purchased from Gene Tools (Philomath, OR, USA). The MO used against *itnp* begins at -5 and runs to ATG at the $+20$ nucleotide position ($5'$ -GACAGCAGACC TCCAGACATTATTC- $3'$). The maximal dosage that caused no obvious toxic effects on embryogenesis was used as follows: *itnp* MO at 1 ng/embryo and mismatched *itnp* MO ($5'$ -GAGAGCACACCTCGAGACAA TAATC- $3'$) at 1 ng/embryo. The MOs were prepared with $1\times$ Danieau solution (58 mM NaCl, 0.7 mM KCl, 0.4 mM MgSO₄, 0.6 mM Ca(NO₃)₂, and 5.0 mM HEPES; pH 7.6). The MO solution (1 ng/embryo) containing 0.1% phenol red (a visualizing indicator) was injected into zebrafish embryos at the 1–2-cell stage using an IM-300 microinjector system (Narishigi Scientific Instrument Laboratory, Tokyo, Japan). Wild-type without injection was only subjected to *itnp* protein measurement and morphological observation. In the subsequent knockdown experiments, mismatched-MO injected embryos were used as the control group.

Enzyme-linked immunosorbent assay (ELISA)

The sequences of zebrafish isotocin [Cys-Tyr-Ile-Ser-Asn-Cys-Pro-Ile-Gly-(NH₂)] and mammalian oxytocin [Cys-Tyr-Ile-Gln-Asn-Cys-Pro-Leu-Gly-(NH₂)] are highly conserved. In order to obtain sufficient amounts of protein, 25 embryos were pooled as a sample. Isolated sample were disrupted in homogenization buffer (100 mM imidazole, 5 mM EDTA, 200 mM sucrose, and 0.1% sodium deoxycholate; pH 7.6), and then centrifuged at 4°C and 10,000 rpm for 10 min. The supernatants were stored at -70°C until further experiments. The proteins were measured by Oxytocin Enzyme Immunoassay Kit (Assay Designs, Ann Arbor, MI, USA). Cross reactivity of the antibody with the synthetic zebrafish isotocin (Kelowna International Scientific Inc., Taipei, Taiwan) was conducted to confirm the quantitative capability of the Oxytocin Enzyme Immunoassay Kit for zebrafish isotocin. Samples that contained 150 μg protein were loaded into each well and incubated at 4°C for 24 h, then the contents of the well were emptied and washed with a wash solution three times. After the final washing, any remaining wash buffer was removed, and the pNpp substrate solution was added to each well. The absorbance was measured at 450 nm in a synergy multi-mode plate reader (BioTek Instruments, Winooski, VT, USA) after stopping the enzymatic reaction by adding stop solution to each well. The standard curve for isotocin was constructed using commercial software (BioTek), and the concentration

of isotocin in unknown samples was determined by interpolation.

Whole-mount in situ hybridization

Fragments of *zatzp6v1a*, *ztrpv6*, *zslc12a10.2*, and *foxi3a* were obtained by PCR and inserted into the pGEM-T easy vector (Promega, Madison, WI, USA). The inserted fragments were amplified with the T7 and SP6 primers by PCR, and the products as templates were used for the in vitro transcription with T7 and SP6 RNA polymerase (Roche) in the presence of digoxigenin (DIG)-UTP (Roche) to, respectively, synthesize sense and anti-sense probes. DIG-labeled RNA probes were examined using RNA gels, and a dot blot assay was used to confirm their quality and concentrations. Zebrafish embryos were anesthetized on ice and fixed with 4% paraformaldehyde in a phosphate-buffered saline (PBS; 1.4 mM NaCl, 0.2 mM KCl, 0.1 mM Na₂HPO₄, and 0.002 mM KH₂PO₄; pH 7.4) solution at 4°C overnight. Afterwards, the samples were washed with diethylpyrocarbonate (DEPC)-treated PBST (PBS with 0.1% Tween-20) several times (for 10 min each). After PBST washing, the samples were incubated with hybridization buffer (HyB, 50% formamide, $5\times$ SSC, and 0.1% Tween 20) at 65°C for 5 min and with HyB containing 500 $\mu\text{g}/\text{ml}$ yeast tRNA at 65°C for 4 h before hybridization. After overnight hybridization with 100 ng/ml DIG-labeled antisense or sense RNA probes, the embryos were serially washed with 50% formamide- $2\times$ SSC (at 65°C for 20 min), $2\times$ SSC (at 65°C for 10 min), $2\times$ SSC (at 65°C for 10 min), $0.2\times$ SSC (at 65°C for 30 min, two times), and PBST at room temperature for 10 min. Afterwards, the embryos were immunoreacted with an alkaline phosphatase-coupled anti-DIG antibody (1:8,000) and stained with nitro blue tetrazolium (NBT) (Roche) and 5-bromo-4-chloro-3-indolyl phosphate (BCIP) (Roche) for the alkaline phosphatase reaction. For the quantification of density, eight areas (85 \times 80 μm each) on the yolk sac surface of an embryo were chosen for counting.

Whole-mount immunohistochemistry

Embryos from different developmental stages were fixed in 4% paraformaldehyde in PBST. Samples were incubated with 3% bovine serum albumin (BSA) for 2 h to block nonspecific binding. Samples were then incubated overnight at 4°C with an $\alpha 5$ monoclonal antibody against the α -subunit of the avian Na⁺-K⁺ ATPase (Developmental Studies Hybridoma Bank, University of Iowa, Ames, IA, USA), and a polyclonal antibody against the α subunit of killifish H⁺ ATPase [37]. In addition, monoclonal anti-human P63 (Santa Cruz Biotechnology, Santa Cruz, CA, USA) was used to label zebrafish epidermal stem cells [35].

After washing with PBST for 20 min, samples were further incubated in Alexa Fluor 488 goat anti-rabbit immunoglobulin (IgG) (Molecular Probes, Carlsbad, CA, USA; 1:200 dilution with PBS) and an Alexa Fluor 568 goat anti-mouse IgG antibody (Molecular Probes; 1:200 dilution with PBST) for 2 h at room temperature. Images were acquired with a Leica TCS-SP5 confocal laser scanning microscope (Leica Lasertechnik, Heidelberg, Germany). The method of cell density quantification was described above.

Plasmid construction

To generate the pCS2⁺-*itnp* constructs, the corresponding *itnp* coding region (465 bp) was PCR-amplified with the following pairs of primers: forward, 5'-GAATT CCGGTGTCAGCCTTGGTGAATAATGTCTG-3'; reverse, 5'-TCTAGAGGCATTTTCATTGGTGGATTCTGGAGGGG-3'; the *itnp* PCR amplicon was cloned into a pGEM-T easy vector (Promega) with *EcoRI* and *XbaI* sites and was then subcloned into a pCS2⁺ vector at the *EcoRI* and *XbaI* sites. The corresponding *EcoRI* and *XbaI* sites are underlined.

Capped-mRNA (cRNA) injection

All constructs cloned in the pCS2⁺ vectors were linearized with *NarI*, and cRNA was transcribed using an SP6 message RNA polymerase kit (Ambion, Huntington, UK). Control embryos were injected with 1× Danieau solution. cRNA was injected into embryos at the 1 to 2-cell stage at 1 ng/embryo.

Statistical analysis

Values are presented as the mean ± SD and were compared using Student's *t* test or one-way analysis of variance (ANOVA, Tukey's pair-wise comparison).

Results

Expression of *itnp* and its receptors in adult zebrafish tissues and embryos

mRNA expressions of the zebrafish *itnp* and its two receptors (*itnpr-like 1* and *itnpr-like 2*; accession number: FJ556869 and FJ556870, respectively) in various tissues were examined by RT-PCR, with β -actin as the internal control. *itnp* mRNA was abundantly expressed in the brain, gills, muscles, and ovaries, and also expressed in the eyes, fins, heart, kidneys, liver, skin, and spleen (Fig. 1a). Both *itnpr-like 1* and *itnpr-like 2* were expressed in a variety of

tissues but with a lower level of *itnpr-like 2* in the eye (Fig. 1a). In zebrafish embryos, *itnp* and the two receptors were first detected at 1 h post-fertilization (hpf), and the expressions were maintained till 72 hpf (Fig. 1b). The RT-PCR analysis was repeated with three different sets of samples, with similar results.

To examine the hypotonic effects on *itnp* expression, 72-hpf embryos were transferred from fresh water to double-deionized water for 24 h, and *itnp* expression levels were measured by qRT-PCR. As shown in Fig. 1c, *itnp* mRNA was significantly upregulated after double-deionized water treatment.

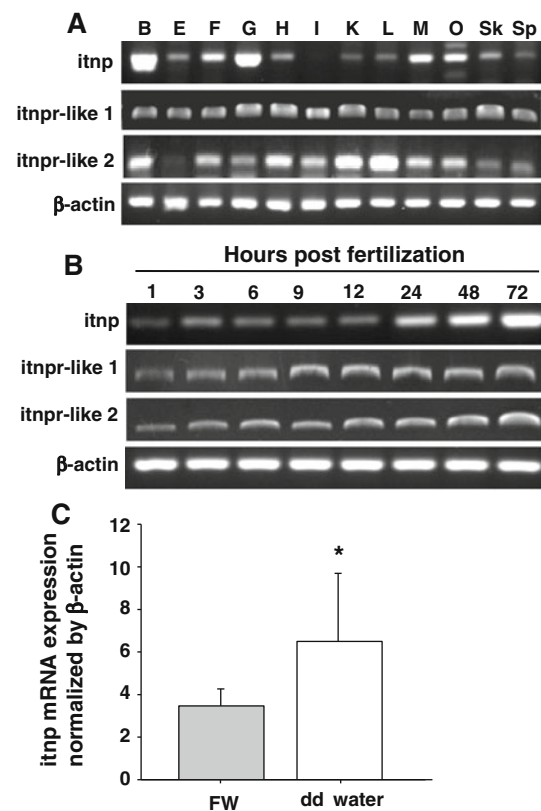


Fig. 1 *itnp* and *itnp* receptor mRNA expression in adult zebrafish tissues and embryos. *itnp*, its receptor (*itnpr-like 1* and *itnpr-like 2*) and β -actin mRNA expression patterns were analyzed by RT-PCR. *itnp* (151 bp), *itnpr-like 1* (211 bp) and *itnpr-like 2* (222 bp) cDNAs were amplified by PCR for 35 cycles and β -actin (173 bp) was amplified for 25 cycles. **a** *itnp* and its receptors were detected in several tissues including the eyes, fins, heart, kidneys, liver, muscles, ovaries, skin, and spleen in adult fish. **b** In zebrafish embryos, *itnp* and its receptors were first detected at 1 hpf, and the expressions were differentially maintained till 72 hpf. **c** *itnp* mRNA expression levels were stimulated after transferring 72-hpf embryos from fresh water to double-deionized water for 24 h. *K* kidney, *Sp* spleen, *L* liver, *M* muscle, *Sk* skin, *G* gill, *H* heart, *B* brain, *I* intestine, *E* eye, *F* fin, *O* ovary

Effects of *itnp* knockdown on *itnp* protein expressions and phenotypes in *itnp* morphants

Figure 1c implies a possible role of isotocin in ion regulation mechanisms in zebrafish. To explore the functional role of isotocin in zebrafish ion regulation, loss- and gain-of-function approaches with *itnp* MO and cRNA were used. To test the specificity and efficiency of the *itnp* MO and cRNA, we compared *itnp* protein concentrations in *itnp* morphants, mismatched-MO (Mis MO)-injected and cRNA-injected embryos by an ELISA. First, we confirmed the quantitative capability of the ELISA kit (Oxytocin Enzyme Immunoassay Kit). Zebrafish isotocin and

mammalian oxytocin showed similar competitive binding curves with the kit (Fig. 2a), indicating the cross-reactivity of the antibody and the quantitative capability of the kit for *itnp* protein measurement.

The *itnp* MO was used to knock down the *itnp* protein expression. In preliminary experiments, we tried several dosages of *itnp* MO (1, 2, and 4 ng/embryo), and found higher dosages (2 and 4 ng) caused higher mortality and abnormal development and body shape. In contrast, the morphants injected with 1 ng MO appeared as wild-type (WT) embryos without injection. The mortality, hatching rate, body length, and body shape between morphants and WT embryos at 72 hpf were similar (Fig. 2c). We therefore

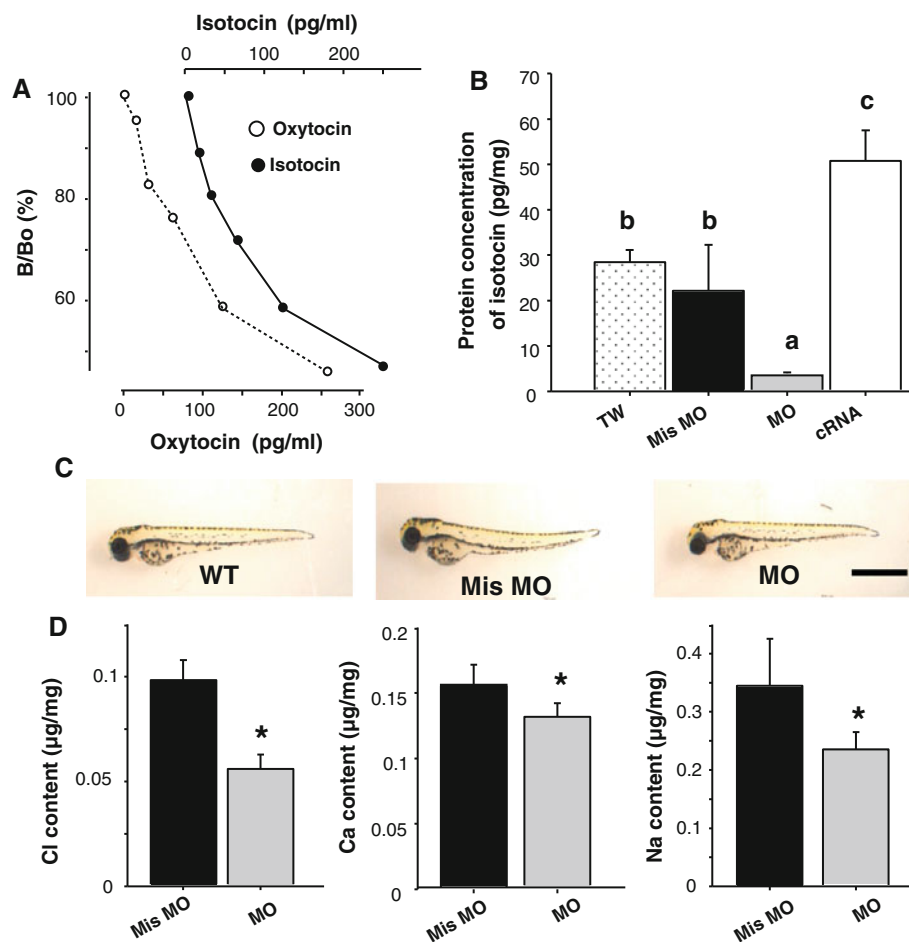


Fig. 2 Effects of knockdown or overexpression of *itnp* on protein expression and phenotypes in zebrafish. **a** Competitive binding curves of synthetic zebrafish isotocin and mammalian oxytocin with the ELISA (Oxytocin Enzyme Immunoassay Kit) showed a similar pattern. **b** One to two-cell stage embryos were injected with *itnp* MO (1 ng/embryo), mismatched-MO (Mis MO), and *itnp* cRNA (1 ng/embryo), and the protein expression at 72 hpf was analyzed by ELISA. *itnp* protein expressions were significantly downregulated in the morphants. In contrast, *itnp* cRNA-injected embryos showed twofold expression of *itnp* protein. No significant difference was found between wild-type (WT) without injection and Mis MO group.

c The morphologies of *itnp* morphants, mismatched-MO-injected embryos, and WT embryos were similar. No significantly different phenotypes were found, suggesting that there were very few side effects in *itnp* morphants. **d** The whole-body contents of Cl^- , Ca^{2+} , and Na^+ were significantly lower in *itnp* morphants than in Mis MO-injected embryos. Values are presented as the mean \pm SD ($n = 5$). Different lowercase letters indicate significant differences (one-way ANOVA, Tukey's pair-wise comparison). Asterisks indicates a significant difference from the Mis MO group (Student's *t* test, $p < 0.05$). Scale bar 500 μm

chose the dosage of 1 ng/embryo to do the subsequent experiments. In this situation, effects of developmental perturbation could be excluded or minimized when the physiological responses induced by *itnp* MO were found. One nanogram of the *itnp* MO and Mis MO were, respectively, injected into 1–2-cell-stage embryos. At 72 hpf, *itnp* protein expression in *itnp* morphants was much lower than those in wild-type and Mis MO-injected zebrafish (Fig. 2b). This result clearly indicated that the *itnp* MO significantly blocked *itnp* protein synthesis. In addition, isotocin protein expression in *itnp* cRNA-injected embryos was twofold higher than that in the wild-type group (Fig. 2b). The morphology of *itnp* morphants, Mis MO-injected embryos, and WT embryos were similar, and no significant phenotype differences were found (Fig. 2c). However, the Cl^- , Ca^{2+} , and Na^+ contents were significantly lower in *itnp* morphants than in Mis MO-injected embryos (Fig. 2d).

Effects of knockdown or overexpression of *itnp* on ionocyte-related gene expressions and ionocyte differentiation

As described above, isotocin appears to be involved in zebrafish ion regulation mechanism. Subsequent loss-of-function experiments were designed to test a hypothesis if isotocin is involved in the development of zebrafish skin/gill ionocytes, which are major cells responsible for ion regulation mechanisms. The mRNA expressions of ionocyte-related genes were downregulated by the *itnp* MO. As shown in Fig. 3a, mRNA expressions of *atp6v1a*, *atp1b1b*, *trpv6*, *slc12a10.2*, and *nhe3b* were reduced in *itnp* morphants. In whole-mount in situ hybridization experiments, RNA signals of *atp6v1a*, *trpv6*, and *slc12a10.2* were also decreased by *itnp* MO knockdown consistent with the qRT-PCR data (Fig. 3b, c). In the whole-mount immunocytochemistry experiments, NaRCs and HRCs were recognized. The cell densities of NaRC and HRC were reduced in *itnp* morphants compared with those in Mis MO-injected embryos (Fig. 4a–c). In contrast, increased cell densities of NaRC and HRC were detected in *itnp*-overexpressed embryos compared with those in the control injected with $1\times$ Danieau solution (Fig. 4d–f).

Since decreases in cell number of different ionocyte subtypes and in expression levels of relevant transporters were observed in *itnp* morphants, we further investigated whether isotocin regulates ionocyte progenitor differentiation. We measured the mRNA expression of *foxi3a*, which was reported to be involved in ionocyte differentiation in zebrafish during early development stages [25–28]. *foxi3a* expression level (Fig. 5a, b) and the number of *foxi3a*-expressing cells (Fig. 5c, e, f) were downregulated by the *itnp* MO and stimulated by *itnp* cRNA at the tail-bud stage

when zebrafish embryos only expressed *foxi3a* but not ion transporter genes, indicating that isotocin affects ionocyte differentiation. The effects on *foxi3a* expression level modulated by *itnp* MO injection or *itnp* overexpression were still observed at the later stage, 3 dpf (Fig. 5a, b).

Effects of knockdown or overexpression of *itnp* on epidermal stem cells in zebrafish embryos

The loss- and gain-of-function approaches were used to further examine if the control pathways of isotocin in ionocyte progenitor differentiation are mediated by regulating epidermal stem cells. P63 is a marker of epithelial stem cells, which were demonstrated to differentiate into skin ionocytes and keratinocytes in zebrafish [35, 36]. To test whether isotocin regulates the number of epidermal stem cells in zebrafish embryos, P63 staining was performed. The density of P63⁺ cells decreased in *itnp* morphants and, on the contrary, increased in *itnp* ectopically expressed embryos (Fig. 6). No difference was found between wild-type and mismatched MO-injected embryos (data not shown).

Discussion

The tissue distribution of mammalian oxytocin was reported [38, 39]. Oxytocin is primarily produced in magnocellular and parvocellular neurons of the hypothalamus, which plays an important role in integrating the vertebrate endocrine system [40]. The biological effects of oxytocin on female reproduction are well known [41]. In addition, oxytocin influences several behavioral and physiological processes such as social and maternal behaviors, learning, memory, steroidogenesis, and muscle contraction [3, 4, 42, 43]. In addition to be expressed in the central nervous system, mRNA was also detected in peripheral tissues including the heart, thymus, uterus, testes, adrenal gland, and ovaries [39], consisting with its wide spectrum of central and peripheral effects. In the present study, zebrafish *itnp* mRNA was detected in various tissues and developing embryos by an RT-PCR analysis (Fig. 1). However, most studies in fish revealed *itnp* mRNA expression in the brain [44–47]; only one paper reported that *itnp* mRNA of the elephant shark was expressed in peripheral tissues [48]. Spatial distribution may differ among species, and further research is required to determine the exact functions of isotocin in these tissues. The highest expression level in the brain which is similar in all vertebrates indicates that the hypothalamus is the main site producing the isotocin peptide. The relative higher expression levels in gills, muscles, and ovaries reveal that isotocin regulates many physiological functions in fish such

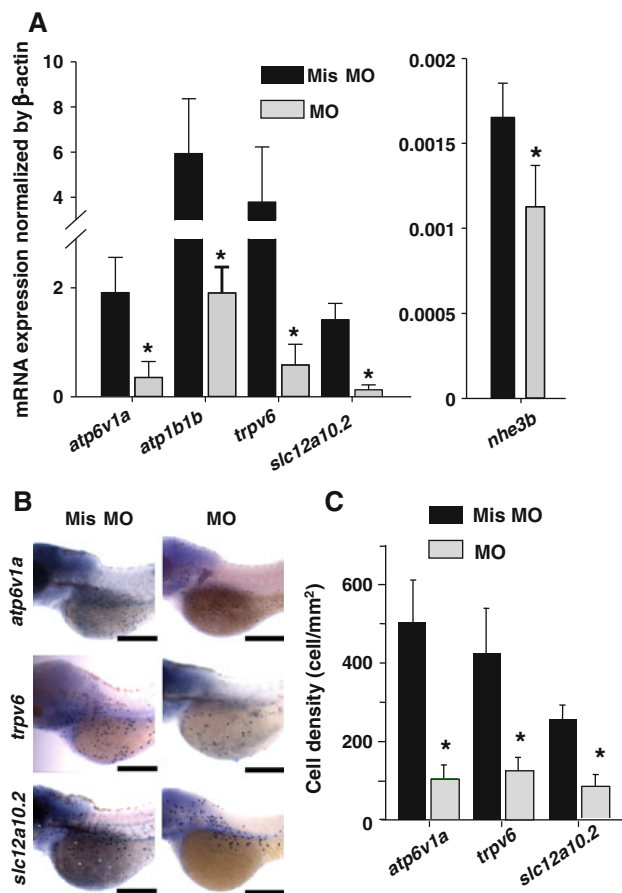


Fig. 3 Effects of *itnp* MO on ionocyte-related gene expressions in zebrafish embryos. One to two-cell stage embryos were injected with *itnp* MO (1 ng/embryo) and a mismatched-MO (Mis MO), respectively, and the mRNA expressions at 72 hpf were analyzed by qRT-PCR. **a** The mRNA expressions of ionocyte-related genes were significantly downregulated by an *itnp* MO injection. **b** In situ hybridization analysis indicated that the mRNA signals of V-ATPase subunit A (*atp6v1a*), epithelial Ca^{2+} channel (*trpv6*), and Na^{+} - Cl^{-} cotransporter (*slc12a10.2*) were lower in *itnp* morphants. **c** Cell densities of *atp6v1a*-, *trpv6*-, and *slc12a10.2*-expressing cells in *itnp* morphants were significantly lower than those in mismatched-MO-injected embryos. qRT-PCR values were normalized to β -actin. Mean \pm SD ($n = 6$). Asterisks indicate a significant difference from the Mis MO group (Student's *t* test, $p < 0.05$). Scale bar 200 μm

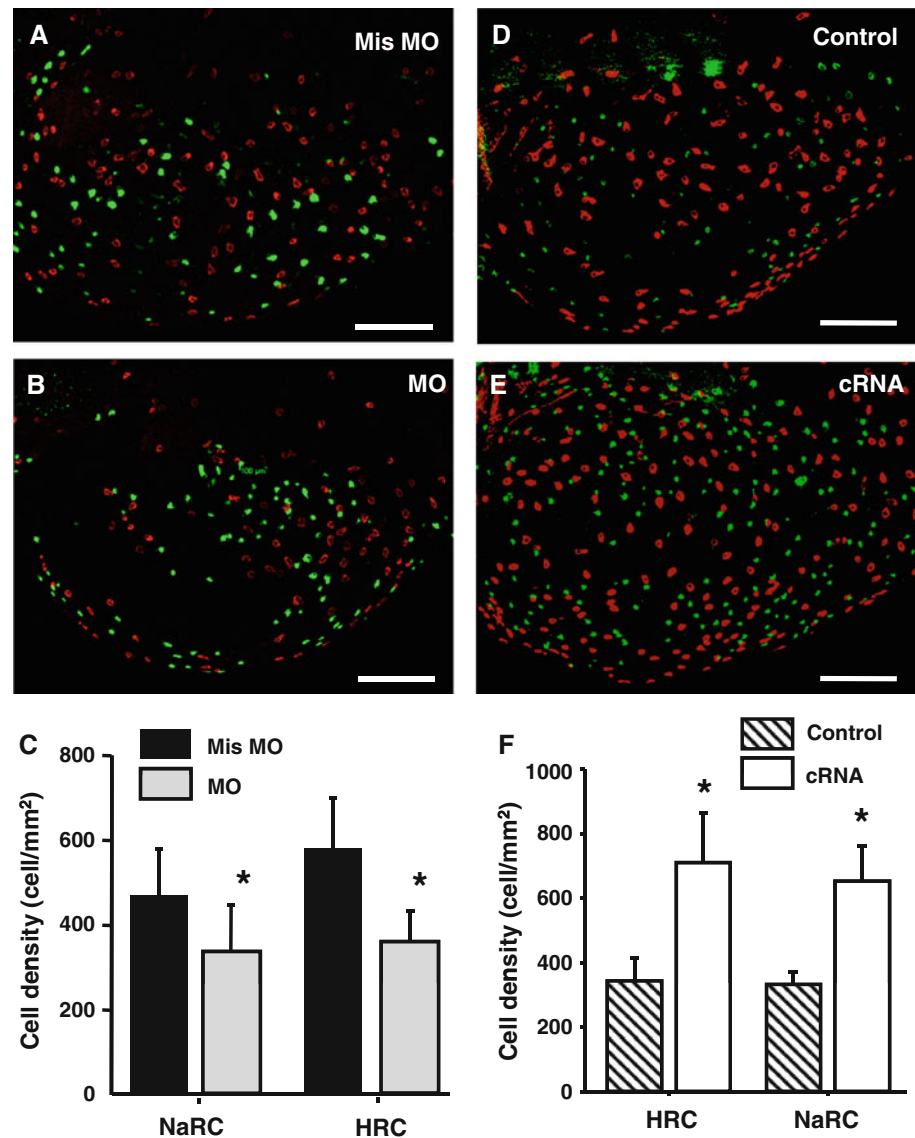
as reproduction and social behavior [49, 50] and support the view that isotocin is synthesized by a paracrine system operating within peripheral tissues [51–53]. It is noted that the transcripts of the two receptors, *itnpr-like 1* and *itnpr-like 2*, were found in all the examined tissues including gill and skin where ionocytes appear, and were initially detected at early developmental stage. The broad expressions of oxytocin/isotocin and its receptors in mammals [39, 54] and fish tissues suggest the conservation and multiple biological actions of these peptides in vertebrates.

In light of body fluid homeostasis, oxytocin was demonstrated to be a modulator like vasopressin, another

neuropeptide. Hyperosmolality results in enhanced oxytocin secretion [39, 55]. Injection of hypertonic saline induced activation of neuronal activities in oxytocinergic cells in mouse hypothalamic paraventricular (PVN) and supraoptic nuclei (SON) [56]. After water deprivation, osmolality and plasma sodium were increased accompanied the elevation of oxytocin mRNA in PVN and SON [57]. The concentration of plasma oxytocin was decreased by water drinking, which caused a signal of osmotic dilution [58]. An oxytocin injection caused increases in urinary osmolality and natriuresis in the rat [59]. In response to hyperosmotic conditions, oxytocin stimulates water uptake and simultaneously reduces Na^{+} reabsorption, which result in downregulation of body fluid osmolality. Likewise, studies on euryhaline teleosts also suggested that isotocin, an ortholog of oxytocin, is associated with hyperosmotic acclimation. In rainbow trout and sea bream, levels of isotocin increased when fish were acclimated to different salinities [60, 61]. Conversely, *itnp* mRNA levels in the pituitary decreased after tiger puffer were transferred from seawater to 10% seawater [47]. In European sea bass, the short-circuit Cl^{-} current increased when isotocin was added to the medium of cultured gill cells [62]. However, knowledge of the mechanisms behind these physiological phenomena is limited due to a lack of information on target cells of isotocin as well as the way in which isotocin controls the functions of target cells. The present study provides molecular physiological data exploring these issues.

In the present study, zebrafish embryos were treated with double-deionized water, and we surprisingly found that *itnp* mRNA expressions were stimulated in an ion-deficient environment (Fig. 1c). In euryhaline teleosts, isotocin was previously found to be induced by hypertonic environments [60]. In contrast, the present findings indicate a role of isotocin in a stenohaline freshwater species during acclimation to a hypotonic situation. Loss-of-function experiments supported this notion. Injection of the *itnp* MO caused lower body ion contents in morphants than those in Mis MO-injected embryos (Fig. 2c). The uptake functions of ions are accomplished by specific ion transporters which are expressed in different types of ionocytes in zebrafish: HRC, NaRC, and NCC [32, 33, 63]. Injection of *itnp* MO significantly decreased mRNA expression level of relevant transporters in ionocytes (Fig. 3) and downregulated cell densities of ionocytes (Figs. 3, 4), providing convincing and direct evidences that skin/gill ionocytes are target cells of isotocin. HRC, NaRC, and NCC were demonstrated to be similar to mammalian kidney proximal tubular cells, distal convoluted cells, and Ca^{2+} -reabsorption cells responsible for Na^{+} , Ca^{2+} , and Cl^{-} uptake, respectively [32, 33]. Therefore, the present study opens a new window for exploring the roles of isotocin (and oxytocin) in

Fig. 4 Effects of *itnp* MO and cRNA on cell densities of NaRC and HRC in zebrafish embryos. One to two-cell stage embryos were injected with the *itnp* MO (1 ng/embryo) (a), a mismatched-MO (Mis MO) (b), 1× Danieau solution (Control) (d), and *itnp* cRNA (1 ng/embryo) (e), respectively, and NaRCs (red) and HRCs (green) were detected by double immunocytochemistry of Na⁺-K⁺-ATPase (red) and H⁺-ATPase (green) at 72 hpf. Cell densities of NaRCs and HRCs in *itnp* morphants were significantly lower than those in mismatched-MO-injected embryos (c), while the cell densities in cRNA-injected embryos were significantly higher than those in the control group (f). Mean ± SD ($n = 5-6$). Asterisks indicate a significant difference (Student's *t* test, $p < 0.05$). Scale bar 100 μm

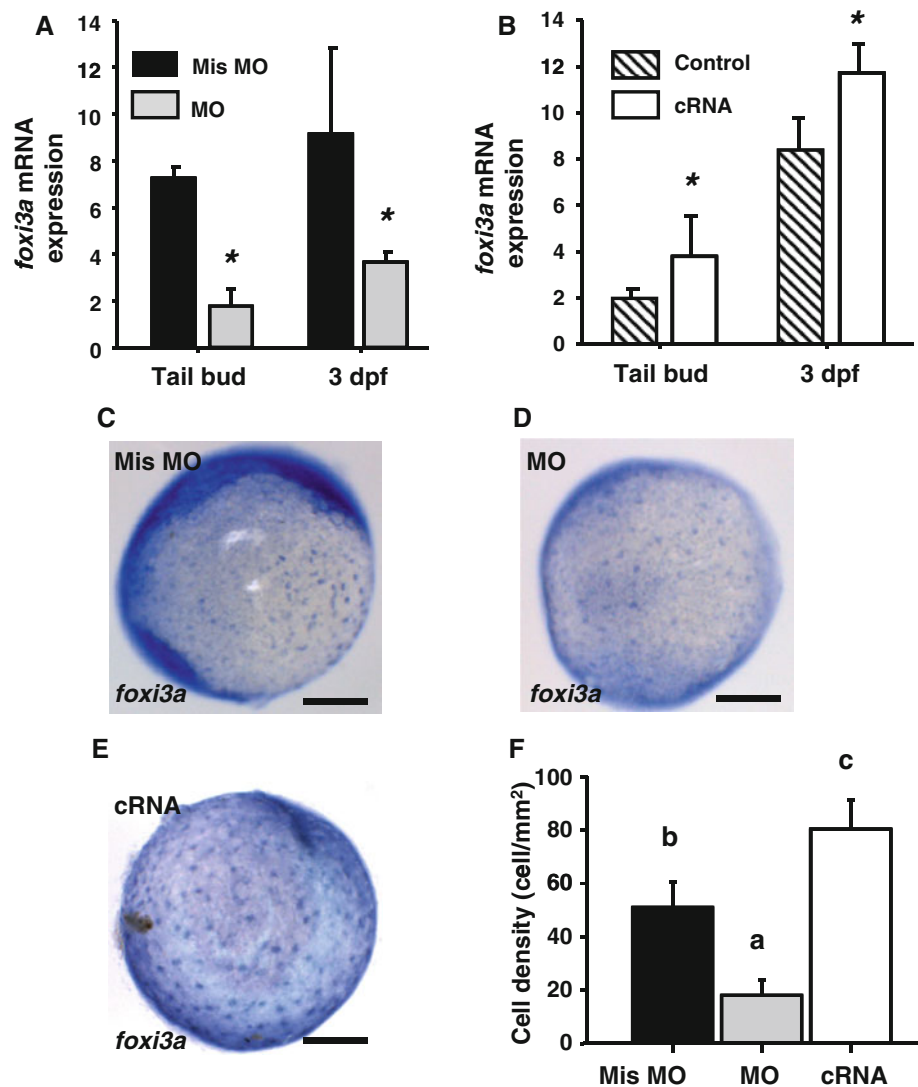


ionoregulatory mechanisms not only in fish but also in mammals.

The numbers and densities of ionocytes are associated with the functional regulation of ion uptake acid/base balance mechanisms in fish during acclimation to environmental changes [19, 32, 33, 64]. The differentiation of ionocytes is regulated by a helix/forkhead box transcription factor, Foxi3a, which functions as a cell fate determinant or cell differentiation regulator [65]. Zebrafish Foxi3a was demonstrated to function as a master regulator of ionocyte differentiation in embryonic stages [25–28, 34]. During zebrafish embryonic development, *foxi3a* starts to be expressed at around the 90% epiboly to tail-bud stages, and the ionocyte markers, *atp1b1b* or *atp6v1a*, are expressed later at the 14–18-somite stages [25]. In the present study, *foxi3a* expression was

significantly suppressed by *itnp* MO and stimulated by *itnp* cRNA at the tail-bud stage when skin ionocytes were not terminally differentiated and remained as progenitors (Fig. 5). On the other hand, overexpression of *itnp* caused increases of NaRC and HRC densities in zebrafish embryos (Fig. 4d–f), similar to the phenotypes of embryos injected with *foxi3a* cRNA [25]. These data indicate that isotocin affects the differentiation of ionocytes by regulating *foxi3a* expression. Moreover, P63⁺ cell densities decreased in *itnp* morphants and inversely increased in the *itnp* cRNA-injected embryos (Fig. 6), suggesting that isotocin may also be involved in stimulating the proliferation of epidermal stem cells. Epidermal stem cells are the source of ionocyte and keratinocyte progenitors. Regulation of epidermal stem cells would modulate ionocyte progenitors and then affect the number of ionocytes.

Fig. 5 Effects of *itnp* MO and cRNA on *foxi3a* expression in zebrafish embryos. One to two-cell stage embryos were injected with the *itnp* MO (1 ng/embryo), a mismatched-MO (Mis MO), *itnp* cRNA (1 ng/embryo) and 1× Danieau solution (Control), respectively, and qRT-PCR analysis of *foxi3a* mRNA expression (a, b) and in situ hybridization for *foxi3a* mRNA (c, d, e, f) in embryos at the tail-bud stage and/or 3 dpf were conducted. *foxi3a* mRNA expression was significantly suppressed by the *itnp* MO (a), but was stimulated by the *itnp* cRNA (b) at both the tail-bud stage and 3 dpf. At the tail-bud stage, the In situ hybridization analysis of *foxi3a* mRNA in *itnp* mismatched-MO (c), *itnp* MO (d), and *itnp* cRNA (e) injected embryos indicated that the density of *foxi3a*-expressing cells was downregulated by *itnp* MO but upregulated by *itnp* cRNA (f). Values were normalized by β -actin. Mean \pm SD ($n = 6$). Asterisks indicate a significant difference from the Mis MO group (Student's *t* test, $p < 0.05$). Different lowercase letters indicate significant differences (one-way ANOVA, Tukey's pair-wise comparison). Scale bar 500 μ m

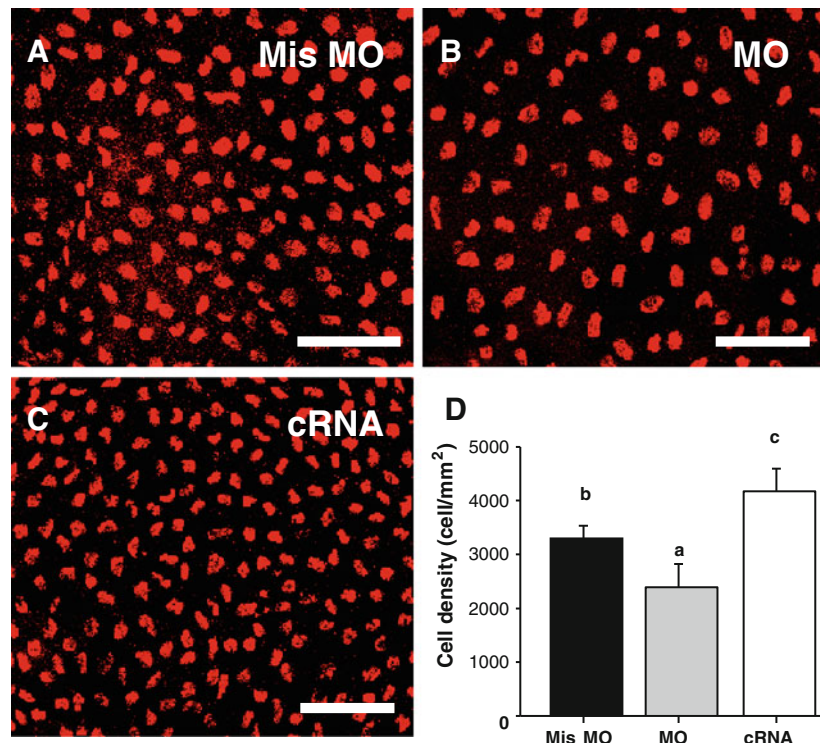


Similarly, the actions of oxytocin on cell differentiation were reported [66]. The oxytocin/oxytocin receptor system exists in the heart, and activation of the cardiac oxytocin receptor stimulates the release of the atrial natriuretic peptide, which lowers blood pressure and promotes cell growth [67]. In cultured mouse P19 embryonic stem cells, incubation of oxytocin stimulated the production of beating cell colonies, while treatment with an oxytocin antagonist, ([d(CH₂)₅, Tyr(Me)², Thr⁴, Orn⁸, Tyr-NH₂⁹] vasotocin) completely inhibited the formation of cardiomyocytes [68]. Oxytocin was also found to be an anabolic bone hormone [18]. Through upregulating *BMP-2* and its downstream molecules, *Schnurri-2* and *-3*, *Osterix*, and *ATF-4*, expressions, oxytocin stimulated osteoblast differentiation to exhibit the mineralizing phenotype [18]. Taken together, isotocin and oxytocin mediate the proliferation and/or differentiation of cells to regulate physiological responses, and this pathway seems to be conserved among vertebrates, thus

indicating a common and important function of these peptides during evolution.

From an osmoregulatory point of view, previous studies proposed that oxytocin and isotocin act as hypertonic hormones to maintain body fluid hydromineral homeostasis; however, molecular mechanisms behind these physiological responses have not been revealed. In contrast, the present study used different approaches to identify target cells of isotocin and discovered a novel mechanism for isotocin to control ion uptake functions. Our data suggest that isotocin plays a role on regulation of the proliferation of epidermal stem cells and differentiation of ionocyte progenitors through mediation by modulating activities of transcription factors, *Foxi3a* and *P63*, to increase ionocyte densities and ultimately regulate the functions of ionocytes. However, more experiments will be necessary to further explore the detailed cellular and molecular mechanisms and to see if this function is direct or indirect.

Fig. 6 Effects of knockdown or overexpression of *itnp* on P63 expression in zebrafish embryos. One to two-cell stage embryos were injected with a mismatched-MO (Mis MO) (1 ng/embryo) (a), *itnp* MO (1 ng/embryo) (b), and isotocin cRNA (1 ng/embryo) (c), respectively, and P63⁺ cells in yolk-sac area were detected by immunocytochemistry at 72 hpf. **d** The density of P63⁺ cells was lower in *itnp* morphants but had increased in *itnp* cRNA-injected embryos. Mean \pm SD ($n = 6$). Different lowercase letters indicate significant differences (one-way ANOVA, Tukey's pair-wise comparison). Scale bar 50 μ m



Acknowledgments This study was financially supported by grants to P. P. Hwang from the National Science Council, and Academia Sinica, Taiwan, ROC. We extend our thanks to Ms. C. C. Lin for her assistance during the experiments and to the Core Facility of the Institute of Cellular and Organismic Biology, Academia Sinica, for assistance with sequencing and microscopy.

Open Access This article is distributed under the terms of the Creative Commons Attribution Noncommercial License which permits any noncommercial use, distribution, and reproduction in any medium, provided the original author(s) and source are credited.

References

- Goodson JL (2008) Nonapeptides and the evolutionary patterning of sociality. *Prog Brain Res* 170:3–15
- Venkatesh B, Brenner S (1995) Structure and organization of the isotocin and vasotocin genes from teleosts. *Adv Exp Med Biol* 395:629–638
- Ferguson JN, Young LJ, Insel TR (2002) The neuroendocrine basis of social recognition. *Front Neuroendocrinol* 23:200–224
- Insel TR, Young L, Wang Z (1997) Central oxytocin and reproductive behaviours. *Rev Reprod* 2:28–37
- Marazziti D, Catena Dell'osso M (2008) The role of oxytocin in neuropsychiatric disorders. *Curr Med Chem* 15:698–704
- Meister B, Villar MJ, Ceccatelli S, Hokfelt T (1990) Localization of chemical messengers in magnocellular neurons of the hypothalamic supraoptic and paraventricular nuclei: an immunohistochemical study using experimental manipulations. *Neuroscience* 37:603–633
- Glass H, Gutkowska J, Favaretto AL, Antunes-Rodrigues J (1997) Correlations between ANP concentrations in atria, plasma and cerebral structures and sodium chloride preference in Wistar rats. *Braz J Med Biol Res* 30:65–68
- Hyodo S, Tsukada T, Takei Y (2004) Neurohypophysial hormones of dogfish, *Triakis scyllium*: structures and salinity-dependent secretion. *Gen Comp Endocrinol* 138:97–104
- Pierson PM, Guibolini ME, Lahlou B (1995) Enzyme linked immunosorbent assay for the neurohypophysial hormones arginine vasotocin and isotocin. *J Immunoassay* 16:55–79
- Warne JM, Hazon N, Rankin JC, Balment RJ (1994) A radioimmunoassay for the determination of arginine vasotocin (AVT): plasma and pituitary concentrations in fresh- and seawater fish. *Gen Comp Endocrinol* 96:438–444
- Warne JM, Hyodo S, Harding K, Balment RJ (2000) Cloning of pro-vasotocin and pro-isotocin cDNAs from the flounder *Platichthys flesus*; levels of hypothalamic mRNA following acute osmotic challenge. *Gen Comp Endocrinol* 119:77–84
- Hausmann H, Meyerhof W, Zwiers H, Lederis K, Richter D (1995) Teleost isotocin receptor: structure, functional expression, mRNA distribution and phylogeny. *FEBS Lett* 370:227–230
- Watanabe Y, Sakihara T, Mukuda T, Ando M (2007) Antagonistic effects of vasotocin and isotocin on the upper esophageal sphincter muscle of the eel acclimated to seawater. *J Comp Physiol B* 177:867–873
- Petersson M (2008) Opposite effects of oxytocin on proliferation of osteosarcoma cell lines. *Regul Pept* 150:50–54
- Geenen V, Kecha O, Brilot F, Charlet-Renard C, Martens H (1999) The thymic repertoire of neuroendocrine-related self antigens: biological role in T-cell selection and pharmacological implications. *Neuroimmunomodulation* 6:115–125
- Sapino A, Macri L, Tonda L, Bussolati G (1993) Oxytocin enhances myoepithelial cell differentiation and proliferation in the mouse mammary gland. *Endocrinology* 133:838–842
- Gassanov N, Devost D, Danalache B, Noiseux N, Jankowski M, Zingg HH, Gutkowska J (2008) Functional activity of the carboxyl-terminally extended oxytocin precursor Peptide during

- cardiac differentiation of embryonic stem cells. *Stem Cells* 26: 45–54
18. Tamma R, Colaianni G, Zhu LL, DiBenedetto A, Greco G, Montemurro G, Patano N, Strippoli M, Vergari R, Mancini L, Colucci S, Grano M, Faccio R, Liu X, Li J, Usmani S, Bachar M, Bab I, Nishimori K, Young LJ, Buettner C, Iqbal J, Sun L, Zaidi M, Zallone A (2009) Oxytocin is an anabolic bone hormone. *Proc Natl Acad Sci USA* 106:7149–7154
 19. Hwang PP, Lee TH (2007) New insights into fish ion regulation and mitochondrion-rich cells. *Comp Biochem Physiol A Mol Integr Physiol* 148:479–497
 20. Tsai JC, Hwang PP (1998) Effects of wheat germ agglutinin and colchicine on microtubules of the mitochondria-rich cells and Ca^{2+} uptake in tilapia (*Oreochromis mossambicus*) larvae. *J Exp Biol* 201:2263–2271
 21. Pan TC, Liao BK, Huang CJ, Lin LY, Hwang PP (2005) Epithelial Ca^{2+} channel expression and Ca^{2+} uptake in developing zebrafish. *Am J Physiol Regul Integr Comp Physiol* 289:R1202–R1211
 22. Liao BK, Deng AN, Chen SC, Chou MY, Hwang PP (2007) Expression and water calcium dependence of calcium transporter isoforms in zebrafish gill mitochondrion-rich cells. *BMC Genomics* 8:354
 23. Horng JL, Lin LY, Huang CJ, Katoh F, Kaneko T, Hwang PP (2007) Knockdown of V-ATPase subunit A (atp6v1a) impairs acid secretion and ion balance in zebrafish (*Danio rerio*). *Am J Physiol Regul Integr Comp Physiol* 292:R2068–R2076
 24. Wang YF, Tseng YC, Yan JJ, Hiroi J, Hwang PP (2009) Role of SLC12A10.2, a Na-Cl cotransporter-like protein, in a Cl uptake mechanism in zebrafish (*Danio rerio*). *Am J Physiol Regul Integr Comp Physiol* 296:R1650–R1660
 25. Hsiao CD, You MS, Guh YJ, Ma M, Jiang YJ, Hwang PP (2007) A positive regulatory loop between foxi3a and foxi3b is essential for specification and differentiation of zebrafish epidermal ionocytes. *PLoS ONE* 2:e302
 26. Esaki M, Hoshijima K, Kobayashi S, Fukuda H, Kawakami K, Hirose S (2007) Visualization in zebrafish larvae of Na^{+} uptake in mitochondria-rich cells whose differentiation is dependent on foxi3a. *Am J Physiol Regul Integr Comp Physiol* 292:R470–R480
 27. Esaki M, Hoshijima K, Nakamura N, Munakata K, Tanaka M, Ookata K, Asakawa K, Kawakami K, Wang W, Weinberg ES, Hirose S (2009) Mechanism of development of ionocytes rich in vacuolar-type H^{+} -ATPase in the skin of zebrafish larvae. *Dev Biol* 329:116–129
 28. Janicke M, Carney TJ, Hammerschmidt M (2007) Foxi3 transcription factors and Notch signaling control the formation of skin ionocytes from epidermal precursors of the zebrafish embryo. *Dev Biol* 307:258–271
 29. Chang WJ, Horng JL, Yan JJ, Hsiao CD, Hwang PP (2009) The transcription factor, glial cell missing 2, is involved in differentiation and functional regulation of H^{+} -ATPase-rich cells in zebrafish (*Danio rerio*). *Am J Physiol Regul Integr Comp Physiol* 296:R1192–R1201
 30. Horng JL, Lin LY, Hwang PP (2009) Functional regulation of H^{+} -ATPase-rich cells in zebrafish embryos acclimated to an acidic environment. *Am J Physiol Cell Physiol* 296:C682–C692
 31. Thisse C, Zon LI (2002) Organogenesis—heart and blood formation from the zebrafish point of view. *Science* 295:457–462
 32. Hwang PP (2009) Ion uptake and acid secretion in zebrafish (*Danio rerio*). *J Exp Biol* 212:1745–1752
 33. Hwang PP, Perry SF (2010) Ionic and acid-base regulation. In: Perry SF, Ekker M, Farrell AP, Brauner CJ (eds) *Fish physiology*. Elsevier Academic Press, San Diego
 34. Janicke M, Renisch B, Hammerschmidt M (2010) Zebrafish grainyhead-like1 is a common marker of different non-keratinocyte epidermal cell lineages, which segregate from each other in a Foxi3-dependent manner. *Int J Dev Biol* 54:837–850
 35. Bakkers J, Hild M, Kramer C, Furutani-Seiki M, Hammerschmidt M (2002) Zebrafish DeltaNp63 is a direct target of Bmp signaling and encodes a transcriptional repressor blocking neural specification in the ventral ectoderm. *Dev Cell* 2:617–627
 36. Lee H, Kimelman D (2002) A dominant-negative form of p63 is required for epidermal proliferation in zebrafish. *Dev Cell* 2: 607–616
 37. Katoh F, Hyodo S, Kaneko T (2003) Vacuolar-type proton pump in the basolateral plasma membrane energizes ion uptake in branchial mitochondria-rich cells of killifish *Fundulus heteroclitus*, adapted to a low ion environment. *J Exp Biol* 206:793–803
 38. Ivell R, Rust W, Einspanier A, Hartung S, Fields M, Fuchs AR (1995) Oxytocin and oxytocin receptor gene expression in the reproductive tract of the pregnant cow: rescue of luteal oxytocin production at term. *Biol Reprod* 53:553–560
 39. Gimpl G, Fahrenholz F (2001) The oxytocin receptor system: structure, function, and regulation. *Physiol Rev* 81:629–683
 40. McCormick SD, Bradshaw D (2006) Hormonal control of salt and water balance in vertebrates. *Gen Comp Endocrinol* 147:3–8
 41. Blanks AM, Thornton S (2003) The role of oxytocin in parturition. *BJOG* 110(Suppl 20):46–51
 42. Filippi S, Morelli A, Vignozzi L, Vannelli GB, Marini M, Ferruzzi P, Mancina R, Crescioli C, Mondaini N, Forti G, Ledda F, Maggi M (2005) Oxytocin mediates the estrogen-dependent contractile activity of endothelin-1 in human and rabbit epididymis. *Endocrinology* 146:3506–3517
 43. Guastella AJ, Mitchell PB, Mathews F (2008) Oxytocin enhances the encoding of positive social memories in humans. *Biol Psychiatry* 64:256–258
 44. Eaton JL, Glasgow E (2007) Zebrafish orthopedia (otp) is required for isotocin cell development. *Dev Genes Evol* 217:149–158
 45. Unger JL, Glasgow E (2003) Expression of isotocin-neurophysin mRNA in developing zebrafish. *Gene Expr Patterns* 3:105–108
 46. Motohashi E, Hamabata T, Ando H (2008) Structure of neurohypophysial hormone genes and changes in the levels of expression during spawning season in grass puffer (*Takifugu niphobles*). *Gen Comp Endocrinol* 155:456–463
 47. Motohashi E, Hasegawa S, Mishihiro K, Ando H (2009) Osmoregulatory responses of expression of vasotocin, isotocin, prolactin and growth hormone genes following hypoosmotic challenge in a stenohaline marine teleost, tiger puffer (*Takifugu rubripes*). *Comp Biochem Physiol A Mol Integr Physiol* 154: 353–359
 48. Gwee PC, Tay BH, Brenner S, Venkatesh B (2009) Characterization of the neurohypophysial hormone gene loci in elephant shark and the Japanese lamprey: origin of the vertebrate neurohypophysial hormone genes. *BMC Evol Biol* 9:47
 49. Popescu JT, Martyniuk CJ, Mennigen J, Xiong H, Zhang D, Xia X, Cossins AR, Trudeau VL (2008) The goldfish (*Carassius auratus*) as a model for neuroendocrine signaling. *Mol Cell Endocrinol* 293:43–56
 50. Goodson JL, Bass AH (2000) Forebrain peptides modulate sexually polymorphic vocal circuitry. *Nature* 403:769–772
 51. Mitchell BF, Fang X, Wong S (1998) Oxytocin: a paracrine hormone in the regulation of parturition? *Rev Reprod* 3:113–122
 52. Nicholson HD, Jenkin L (1995) Oxytocin and prostatic function. *Adv Exp Med Biol* 395:529–538
 53. Jankowski M, Wang D, Hajjar F, Mukaddam-Daher S, McCann SM, Gutkowska J (2000) Oxytocin and its receptors are synthesized in the rat vasculature. *Proc Natl Acad Sci USA* 97: 6207–6211
 54. Struneka A, Hynie S, Klenerova V (2009) Role of oxytocin/oxytocin receptor system in regulation of cell growth and neoplastic processes. *Folia Biol* 55:159–165

55. Gomes DA, Giusti-Paiva A, Ventura RR, Elias LL, Cunha FQ, Antunes-Rodrigues J (2009) Carbon monoxide and nitric oxide modulate hyperosmolality-induced oxytocin secretion by the hypothalamus in vitro. *Biosci Rep* 30:351–357
56. Pirmik Z, Mravec B, Kiss A (2004) Fos protein expression in mouse hypothalamic paraventricular (PVN) and supraoptic (SON) nuclei upon osmotic stimulus: colocalization with vasopressin, oxytocin, and tyrosine hydroxylase. *Neurochem Int* 45: 597–607
57. da Silveira LT, Junta CM, Monesi N, de Oliveira-Pelegri GR, Passos GA, Rocha MJ (2007) Time course of c-fos, vasopressin and oxytocin mRNA expression in the hypothalamus following long-term dehydration. *Cell Mol Neurobiol* 27:575–584
58. Huang W, Sved AF, Stricker EM (2000) Water ingestion provides an early signal inhibiting osmotically stimulated vasopressin secretion in rats. *Am J Physiol Regul Integr Comp Physiol* 279: R756–R760
59. Haanwinckel MA, Elias LK, Favaretto AL, Gutkowska J, McCann SM, Antunes-Rodrigues J (1995) Oxytocin mediates atrial natriuretic peptide release and natriuresis after volume expansion in the rat. *Proc Natl Acad Sci USA* 92:7902–7906
60. Kulczykowska E (1997) Response of circulating arginine vasotocin and isotocin to rapid osmotic challenge in rainbow trout. *Comp Biochem Physiol A Mol Integr Physiol* 118:773–778
61. Kleszczynska A, Vargas-Chacoff L, Gozdowska M, Kalamarz H, Martinez-Rodriguez G, Mancera JM, Kulczykowska E (2006) Arginine vasotocin, isotocin and melatonin responses following acclimation of gilthead sea bream (*Sparus aurata*) to different environmental salinities. *Comp Biochem Physiol A Mol Integr Physiol* 145:268–273
62. Guibbolini ME, Avella M (2003) Neurohypophysial hormone regulation of Cl^- secretion: physiological evidence for V1-type receptors in sea bass gill respiratory cells in culture. *J Endocrinol* 176:111–119
63. Liao BK, Chen RD, Hwang PP (2009) Expression regulation of Na^+/K^+ -ATPase alpha1-subunit subtypes in zebrafish gill ionocytes. *Am J Physiol Regul Integr Comp Physiol* 296:R1897–R1906
64. Evans DH, Piermarini PM, Choe KP (2005) The multifunctional fish gill: dominant site of gas exchange, osmoregulation, acid-base regulation, and excretion of nitrogenous waste. *Physiol Rev* 85:97–177
65. Solomon KS, Logsdon JM Jr, Fritz A (2003) Expression and phylogenetic analyses of three zebrafish FoxI class genes. *Dev Dyn* 228:301–307
66. Hatami L, Valojerdi MR, Mowla SJ (2007) Effects of oxytocin on cardiomyocyte differentiation from mouse embryonic stem cells. *Int J Cardiol* 117:80–89
67. Jankowski M, Hajjar F, Kawas SA, Mukaddam-Daher S, Hoffman G, McCann SM, Gutkowska (1998) Rat heart: a site of oxytocin production and action. *Proc Natl Acad Sci USA* 95:14558–14563
68. Paquin J, Danalache BA, Jankowski M, McCann SM, Gutkowska J (2002) Oxytocin induces differentiation of P19 embryonic stem cells to cardiomyocytes. *Proc Natl Acad Sci USA* 99:9550–9555